





ORIGINAL ARTICLE

# Desorption isotherms and isosteric heat of protein hydrolysate from tilapia slaughtering by-product

*Isotermas de dessorção e calor isostérico do hidrolisado proteico do subproduto de abate de tilápia*

Júlio Cesar Adams Haab<sup>1</sup> , Gracielle Johann<sup>2\*</sup> , Edson Antonio da Silva<sup>1</sup> ,  
Melissa Gurgel Adeodato Vieira<sup>3</sup> 

<sup>1</sup>Universidade Estadual do Oeste do Paraná (UNIOESTE), Curso de Engenharia Química, Toledo/PR - Brasil

<sup>2</sup>Universidade Tecnológica Federal do Paraná (UTFPR), Curso de Engenharia de Bioprocessos e Biotecnologia, Dois Vizinhos/PR - Brasil

<sup>3</sup>Universidade Estadual de Campinas (UNICAMP), Escola de Engenharia Química, Campinas/SP - Brasil

\*Corresponding Author: Gracielle Johann, Universidade Tecnológica Federal do Paraná (UTFPR), Curso de Engenharia de Bioprocessos e Biotecnologia, Estrada para Boa Esperança, Km 04, CEP 85660-000, Dois Vizinhos/PR - Brasil, e-mail: grajohann@gmail.com

**Cite as:** Haab, J. C. A., Johann, G., Silva, E. A., & Vieira, M. G. A. (2022). Desorption isotherms and isosteric heat of protein hydrolysate from tilapia slaughtering by-product. *Brazilian Journal of Food Technology*, 25, e2021169. <https://doi.org/10.1590/1981-6723.16921>

## Abstract

Due to the by-products generated during the processing of meat, biomolecules derived from these by-products, in the form of protein hydrolysates, have been studied for being used as raw materials to produce food. In the present study, the tilapia slaughtering by-products were hydrolyzed, under 60 °C for 2 hours, and spray-dried under 130 °C. After the drying process, equilibrium isotherms of the by-products were obtained through the dynamic method, under temperatures of 20 °C, 35 °C, and 50 °C. All the equilibrium curves presented type III behavior and in the adjustment of the empirical models, the White and Eyring model represented more properly the experimental data of equilibrium. This model presented the highest value of the determination coefficient and lower values of the Sum of the Squares of Residuals (SSR), Relative Mean Error (RME), and Akaike Information Criteria (AIC). The isosteric desorption heat, calculated by the Othmer method, varied from 2395 to 5682 kJ/kg, for equilibrium moisture contents between 0.09 and 0.30 kg/kg. The equation obtained for the calculation of the isosteric desorption heat of the tilapia by-product hydrolysate can be employed in calculations related to the modeling, simulation, optimization, and control of industrial-scale drying processes.

**Keywords:** Drying; Desorption heat; Fish; Storage.

## Resumo

Durante o processamento de carne, subprodutos são gerados. Biomoléculas derivadas desses subprodutos, na forma de hidrolisados proteicos, estão sendo estudadas para sua utilização como matéria-prima na produção de alimentos. No presente estudo, os subprodutos do abate da tilápia foram hidrolisados a 60 °C por 2 h e secos por atomização a 130 °C. Após o processo de secagem, foram obtidas isotermas de equilíbrio para os subprodutos pelo método dinâmico, nas temperaturas de 20 °C, 35 °C e 50 °C. Todas as curvas de equilíbrio apresentaram comportamento do tipo III e, no ajuste dos



This is an Open Access article distributed under the terms of the Creative Commons Attribution License, which permits unrestricted use, distribution, and reproduction in any medium, provided the original work is properly cited.

modelos empíricos, o modelo de White e Eyring representou mais adequadamente os dados experimentais de equilíbrio. Este modelo apresentou o maior valor do coeficiente de determinação e os menores valores da soma dos quadrados dos resíduos, erro médio relativo e Critérios de Seleção de Akaike. O calor isostérico de dessorção, calculado pelo método de Othmer, variou entre 2.395 e 5.682 kJ/kg, para teores de umidade de equilíbrio entre 0,09 e 0,30 kg/kg. A equação obtida para o cálculo do calor isostérico de dessorção do hidrolisado do subproduto da tilápia pode ser empregada em cálculos relacionados a modelagem, simulação, otimização e controle de processos de secagem em escala industrial.

**Palavras-chave:** Secagem; Calor de dessorção; Peixe; Armazenamento.

## Highlights

The White and Eyring model is suitable for predicting the desorption data of NT by-product

The energy required during the NT by-product drying was achieved by Othmer method

The results are useful for drying design, predicting energy demand and storage conditions

## 1 Introduction

Due to growing aquaculture production, only in the year 2018, around 179 million tons of fish were produced worldwide (Food and Agriculture Organization of the United Nations, 2020). The demand for fish protein, essential amino acid, and fatty acid grows along with the population throughout the world as well as its preference for fish and the health advantages associated with its consumption (Desai et al., 2018; Kobayashi & Park, 2018). In this group is the tilapia, a common designation of cichlids fish species, found in America, Asia and Africa, where it can be considered the most important freshwater fish (Al-Deghayem et al., 2017). Although 22 species are commercially grown, Nile tilapia (*Oreochromis niloticus*), NT, represents 90% of the commercial production (Miranda et al., 2010). This production generates a large amount of by-product, mainly composed of viscera, head, skin, bone, and muscle tissue (Shu & Tsai, 2016), which represents a significant volume of raw material that is rich in proteins and fatty acids from the omega-3 series (Feltes et al., 2010; Zapata & De La Pava, 2018).

In this sense, the increasing amount of food by-products originated by modern society represent not only a resource problem but also an environmental and economic problem besides being a moral challenge. The generation of huge volumes of by-products from animal slaughtering leads to the development of new processes for the treatment and exploitation of these by-products. It can produce alternative sources, preserve the environment, and evolve in the attendance of more demanding environmental laws. Regarding animal slaughtering by-products management, like the NT, one practice that has been highlighted is the extraction, isolation, and use of biomolecules originating from these by-products. The obtainment of a protein hydrolysate, for use as a raw material to produce pet and human food, represents a possibility of value aggregation.

However, due to the high contents of water and protein, the hydrolysate is very susceptible to decomposition. One option is to subject it to the most common meat preservation technique, *i.e.*, drying technique (Chabbouh et al., 2013). Although, for further use of protein hydrolysate in drying industrial scale, techniques of modeling and simulation are indispensable. Without them, the project, control, and optimization of unit operations are unfeasible. Still, only with the previous knowledge of the desorption isotherms and the isosteric heat is possible to design a drying system. These thermodynamic properties are essential in processes that involve simultaneous heat and mass transfer, as drying operations. Desorption isotherms are unique for each product (Galdeano et al., 2018) and very important, since, once the breakeven point is known, it can estimate the time needed to reach it, avoiding unnecessary energy expenditure during the drying operations, and provide information about the safe moisture contents (Botelho et al., 2019). In turn, isosteric heat is considered an essential parameter in energy demanded on drying processes because it is related to the amount of energy to remove the free water (Oliveira et al., 2017).

In the literature, there are some works that evaluated the equilibrium isotherms for hydrolysates produced from aquatic meat products, such as Antarctic krill meat (Zhang et al., 2002), horse mackerel, chub mackerel, white croaker, sardine, and flying fish (Khan et al., 2003), as well as NT meat (Candido & Sgarbieri, 2003), and mussel meat (Silva et al., 2012). However, there is only one paper that evaluated the isosteric heat of tilapia viscera (Camaño Echavarría et al., 2021) and there are no studies that evaluated the equilibrium isotherms and isosteric heat of the NT slaughtering by-products. So, the present work aimed at obtaining of the desorption isotherms and the calculation of the isosteric heat of the protein hydrolysate produced from NT slaughtering by-products. This evaluation allowed the application of the obtained data in studies of modeling, simulation, and optimization of the dried NT slaughtering by-product protein hydrolysate production and storage for commercial use.

## 2 Material and methods

The tilapia slaughtering by-product, composed of head, spine, and tail, was collected after the fish processing in the Tilapia Brazilian slaughterhouse of the municipality of Toledo (24° 43' 12" S; 53° 44' 36" W, and altitude of 550 m). The experimental procedure for the hydrolysis followed in this work was identical to that described by Dieterich et al. (2014). The by-product was cooled at approximately 5 °C at the facility, packed in thermal boxes, and immediately taken to the laboratory, where the hydrolysis took place. Approximately 2 h elapsed from slaughter to hydrolysis. The by-product, still fresh, was ground in an electric grinder and hydrolyzed in a 5 kg bench reactor. The hydrolysis was carried out with a proteolytic enzyme from *Bacillus licheniformis* (Alcalase® 2.5L, Novozymes) in a 5 L Pyrex beaker, under an aqueous medium, with 15% of water and 0.2% of enzyme (related to the total mass of by-product from NT). For heating, a common kitchen burner powered by LPG was used under 60 °C and continuously stirred (350 rpm) by a mechanical stirrer (Marconi MA-03) for 2 h. After this process, the reaction was interrupted by keeping the temperature of the reactive medium at 90 °C for 20 min. The product was then filtered, bottled, and cooled to 8 °C.

Seeing that it was produced from a greasy raw material, the NT by-product protein hydrolysate presents a high oil content, of approximately 15% (Schössler et al., 2012). That oil, when heated inside the spray dryer, tends to adhere to the walls of the drying chamber, thus reducing yield and affecting the quality of the dehydrated product. Then, the raw hydrolysate was centrifuged in bench equipment ROTINA 420 from HETTICH, for 15 min at 8000 rpm. The supernatant oil was removed from the bottles manually. The remaining contents (protein and aqueous phases) were stirred until re-composition and then fed into the dryer.

The protein content determination of the hydrolysate was carried out in duplicate, according to the methodology of AOAC (Association of Official Analytical Chemists, 1995). The analysis was conducted at the Food Quality Laboratory (LQA) at *Universidade Estadual do Oeste do Paraná* (UNIOESTE) campus Toledo.

The hydrolysates were dried on an MSD 1.0 bench spray dryer from LABMAQ of Brazil, at the facilities of the Food Centre Laboratory from the Federal Technological University of Paraná – Medianeira. This equipment is composed of a drying chamber and cyclone built-in stainless steel. The operating procedure consisted of turning on the air blower at the minimum flow rate of 20 L/min. The electric resistance was turned on to keep the initial temperature at 70 °C. The drying air temperature was increased by 10 °C steps until reaching 100 °C, when was started the feeding of water at a flow rate of 0.21 L/h. Then, the temperature was raised to 130 °C, when the product feed was initiated. The feeding is provided by a peristaltic pump, with a flow rate capacity from 0.2 to 1.0 L/h. The maximum inlet drying air temperature used was 200 °C.

The air circulation system is composed of a 500 W air blower and a 3500 W electric resistance. The drying chamber has 50 cm in height and a diameter of 20 cm. The atomization of the liquid feed is obtained through

a pressurized double fluid nozzle. The liquid feed is mixed with compressed air before the injection on the nozzle. This mixture is then forced through the orifice on the nozzle, creating a fog (spray) inside the drying chamber. For the experiments described a nozzle with an orifice of 1.2 mm in diameter was used. The dried product passes through the cyclone, where the hot and moist air is expelled from the top and the powder is collected in a glass bottle at the bottom. After the spray-drying, 0.1 g samples were dried in a vacuum kiln brand Quimis, model Q819V2, at 70 °C for 24 h, and kept in a desiccator until room temperature was reached.

For the desorption isotherm experiment, firstly the samples were humidified until 95% in a Dynamic Vapor Sorption (DVS) equipment made by Surface Measurement Systems (SMS) model DVS 002. The equipment belongs to the Analytical Resources and Calibration Laboratory of the Chemical Engineering Faculty of the State University of Campinas – São Paulo, Brazil. The equipment has a microbalance, that measures the moisture loss of the sample, by dragging an inert gas, with relative humidity and controlled temperature. Moisture was generated from mass flow drivers, mixing the flows of dry gas and saturated steam in certain proportions, to obtain the desired relative humidity. After the samples reached 95% of relative humidity, the experimental desorption run atomically started inside the DVS. The desorption isotherms were obtained in the range of 95 to 0% (in 10.6% step) of relative humidity, at temperatures of 20 °C, 35 °C, and 50 °C (Wani & Kumar, 2016). The moisture content of hydrolysates samples was measured according to the AOAC method (Association of Official Analytical Chemists, 1995).

The equilibrium moistures were calculated in dry base (d.b.) and then the isotherms were drawn according to the water activity, for each one of the three experimental temperatures. The models presented in this work are in Table 1, where  $X_E$  is the equilibrium moisture content, d.b.,  $a_W$  is the water activity, A, B, C, and k are model parameters, and  $X_m$  is the monomolecular moisture content, d.b.

**Table 1.** Mathematical models for fitting the desorption isotherms.

Model	Equation
Langmuir (Langmuir, 1916)	$X_E = \frac{A B a_W}{1 + B a_W}$
White and Eyring (White & Eyring, 1947)	$X_E = \frac{1}{A + B a_W}$
Caurie (Caurie, 1970)	$X_E = \exp(A + B a_W)$
Chirife and Iglesias (Chirife & Iglesias, 1978)	$X_E = A + B \left( \frac{a_W}{1 - a_W} \right)$
Oswin (Oswin, 1946)	$X_E = A \left( \frac{a_W}{1 - a_W} \right)^B$
Smith (Smith, 1947)	$X_E = A - B \ln(1 - a_W)$
Brunauer–Emmett–Teller (BET) (Brunauer et al., 1938)	$X_E = \frac{X_m C a_W}{(1 - a_W)[1 + (C - 1)a_W]}$
Guggenheim–Anderson–De Boer (GAB) (Van der Berg & Bruin, 1981)	$X_E = \frac{X_m C K a_W}{(1 - K a_W)[1 + (C - 1)K a_W]}$

Using the Maple 13<sup>®</sup> software, the parameters of the models were estimated, applying the NonlinearFit command, Modified Newton method with a converging criterion of  $10^{-11}$ .

For the representativeness analysis of the desorption models, statistical tests of determination coefficient ( $R^2$ ), Sum of Squares of Residues (SSR), Relative Mean Error (RME), and Akaike Information Criteria (AIC) were used.

The isosteric heat of desorption can be defined as the total heat of desorption minus the latent heat of vaporization of pure water at the system temperature, Equation 1:

$$q_{st} = Q_{st} - \dot{e}_V \quad (1)$$

where:

$q_{st}$  – isosteric heat of desorption, kJ/kg;

$Q_{st}$  – total heat of desorption, kJ/kg; and,

$\ddot{e}_V$  – latent heat of vaporization of pure water at the system temperature, kJ/kg.

According to Brooker et al. (Brooker et al., 1992), the latent heat of vaporization of pure water is defined by Equation 2, valid for  $273.15 < T_{ABS} < 338.72$ :

$$\ddot{e}_V = 2.503 \times 10^3 - 2.386(T_{ABS} - 273.15) \quad (2)$$

where:

$T_{ABS}$  - absolute temperature, K.

There are several methods to obtain the isosteric heat of desorption, being the Clausius-Clapeyron equation the most extensively used, relating the changes in water activity with temperature. An alternative method was developed by Othmer (Othmer & Brown, 1940), which assumes that the isosteric heats of desorption and condensation have the same functional dependency with temperature.

The Othmer Equation establishes that, once the equilibrium moisture,  $X_E$ , is known in different temperatures and vapor pressures,  $P_V$ , and in known values of partial pressures,  $P_P$ , the relation between the heat of vaporization of pure water,  $\ddot{e}_V$ , and the total heat of desorption,  $Q_{st}$ , can be determined. Thus, from an equilibrium liquid-vapor system, the relationship is defined by Equation 3:

$$\left( \frac{\partial \ln P_V}{\partial \ln P_P} \right)_{X_E} = \frac{Q_{st}}{\ddot{e}_V} \quad (3)$$

where:

$P_V$  – vapor pressure, Pa; and

$P_P$  – partial pressure.

To achieve the heat of desorption of NT slaughtering by-product protein hydrolysate,  $Q_{st}$ , the water activity,  $a_W$ , was computed using an equilibrium moisture content value,  $X_E$ , from a suitable isotherm. This procedure was repeated for each experimental temperature (20 °C, 35 °C, and 50 °C), when also the vapor pressure,  $P_V$ , was evaluated. Finally, the partial pressure,  $P_P$ , was obtained from the values of  $a_W$  and  $P_V$ . This procedure was repeated using different equilibrium moisture content (Djendoubi et al., 2009; Toujani et al., 2011), since according to the Othmer Method the ratio total heat of desorption and heat of vaporization of pure water,  $Q_{st}/\ddot{e}_V$ , is temperature-independent, varying only with the equilibrium moisture content. The value  $Q_{st}/\ddot{e}_V$  was determined from the slope after plotting  $\ln P_V$  versus  $\ln P_P$  at constant  $X_E$ . The relationship between  $Q_{st}$  and  $X_E$  was found by regression technique.

### 3 Results and discussion

After the hydrolysis process, the protein hydrolysate obtained presented an average protein content of 79.18% and moisture content of 0.126 d.b. The adjusted model parameters to the desorption isotherms from the protein hydrolysate are presented in Table 2. In Table 3, the statistical analysis is presented based on the experimental data and those obtained by simplified desorption models. Although the experimental range was from 0.95 to 0.0  $a_W$ , the model's fit was done in the range 0.739 to 0.0  $a_W$ . The other values were not considered while evaluating the results, when using all the experimental points with the fits which had less accuracy. This fact could be attributed to the difficulties in conducting measurements at high aw, which implies low water diffusion and high time to reach the equilibrium (Leuk et al., 2016).

**Table 2.** Adjusted model parameters to the desorption isotherms.

Models	A			B			Xm			C			K		
	20 °C	35 °C	50 °C	20 °C	35 °C	50 °C	20 °C	35 °C	50 °C	20 °C	35 °C	50 °C	20 °C	35 °C	50 °C
Langmuir	1.744	1.833	2.453	0.290	0.219	0.135	-	-	-	-	-	-	-	-	-
White and Eiring	11.473	16.375	18.403	-12.064	-18.252	-20.210	-	-	-	-	-	-	-	-	-
Caurie	-2.695	-3.297	-3.436	2.238	2.906	2.881	-	-	-	-	-	-	-	-	-
Iglesias and Chirife	0.091	0.054	0.044	0.100	0.097	0.084	-	-	-	-	-	-	-	-	-
Oswin	0.088	0.057	0.050	1.097	0.057	1.307	-	-	-	-	-	-	-	-	-
Smith	0.074	0.037	0.028	-0.197	-0.169	-0.169	-	-	-	-	-	-	-	-	-
BET	-	-	-	-	-	-	0.096	0.085	0.074	6.26E+06	10.685	8.960	-	-	-
GAB	-	-	-	-	-	-	0.084	-0.060	0.057	5.53E+08	1.000	55.243	1.063	-7.23E+03	55.243

**Table 3.** Statistical evaluation of the adjusted models to the experimental data of the equilibrium isotherms.

Models	R <sup>2</sup>	SSR	RME (%)	AIC
Langmuir	0.674	1.165	34.23	-9.422
White and Eyring	0.987	0.055	6.37	-35.988
Caurie	0.918	0.370	17.74	-18.850
Iglesias and Chirife	0.975	0.091	9.00	-30.895
Oswin	0.984	0.160	6.96	-25.426
Smith	0.889	0.407	19.10	-17.953
BET	0.860	1.131	22.16	-9.657
GAB	0.887	1.037	17.29	-10.351

According to the results in Table 3, it was possible to verify that the models which better adjusted to the experimental data were the White and Eyring and Oswin. These models presented the highest value of the determination coefficient ( $R^2$ ) 0.987 and 0.984, and lower values of RME between 6.37 and 6.96, respectively for White and Eyring and Oswin model.

In the Figures 1A and 1B are presented the residue distribution for White and Eyring and Oswin models, which showed the deviation between the observed and the model estimated values.

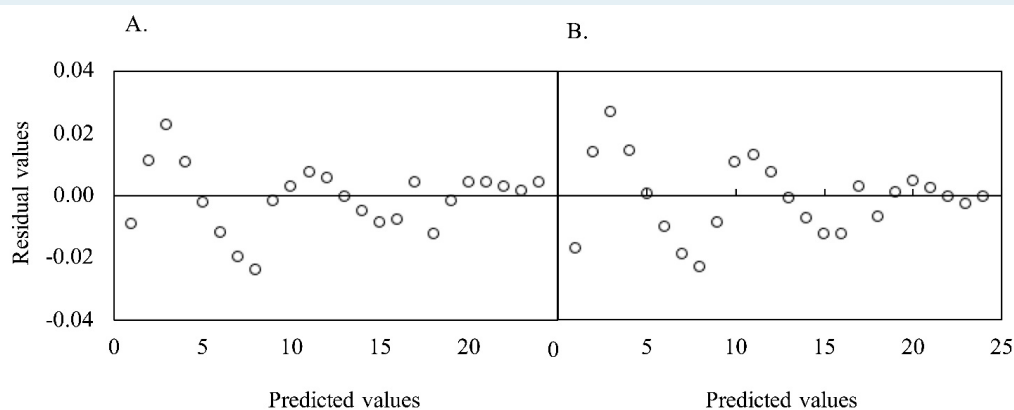


**Figure 1.** Residue distributions for White and Eyring (A) and Oswin models

Regarding Figures 1A and 1B, we can see that both models presented a random distribution of residues and were adequate to represent the tilapia slaughtering by-product protein hydrolysate desorption isotherm. With similar goodness of fit test, the AIC can be used as an additional parameter to select the best model. As the lower AIC values indicated a better fit of the model, the values of -35.988 and -25.426 (Table 3), respectively for White and Eyring and Oswin model, allowed us to take the White and Eyring model as the best in predicting the desorption isotherms from NT slaughtering by-product protein hydrolysate.

The White and Eyring model had a similar form to the Oswin model. This Oswin model was developed for sigmoidal curves and is the best empirical model for predicting protein isotherms (Ibarz & Barbosa-Canovas, 2014) in addition to being suitable for a wide range of isotherms. However, when tested, the Oswin model showed a slightly lesser fit compared to the White and Eyring model. This model is suitable for high values of water activity (Ibarz & Barbosa-Canovas, 2014) and materials of long-chain chemicals (Jian & Jayas, 2021).

In Figure 2 is illustrated the experimental desorption data of the protein hydrolysate of NT slaughtering by-product, as well as the adjustment of the White and Eyring and Oswin models to the experimental data.

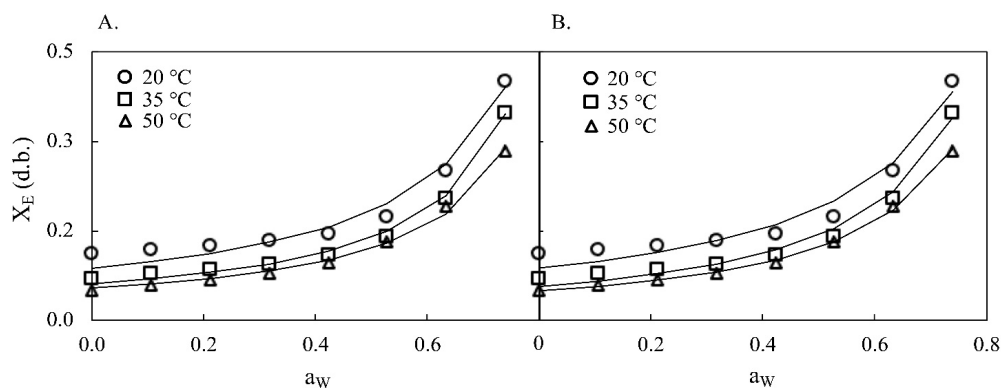


**Figure 2.** White and Eyring (A) and Oswin (B) models adjustment to the experimental equilibrium data.

According to Figure 2, it could be verified that all the desorption curves were concave and presented a type III isotherm, that behavior is non-sigmoidal (J shape) according to the BET classification (Brunauer et al., 1940). This type of isotherm is common for foods with water-soluble solids (Marques et al., 2022), in which the solid matrix adsorbs small amounts of water at low water activity,  $a_w$ , and large quantities of water at high water activity (Blahovec & Yanniotis, 2009). When  $a_w$  is low, the equilibrium moisture content,  $X_E$ , increases linearly with  $a_w$ , and when  $a_w$  is high, the equilibrium moisture content,  $X_E$ , of the solid increases exponentially, due to the formation of capillary condensation region (Bastioğlu et al., 2017). This step is clear in Figure 2 for  $a_w > 0.4$ . When  $a_w \sim 0.6$ , in which the food is considered dried (Moreira et al., 2005), if the temperature rises from 20 °C to 50 °C, the  $X_E$  value must be reduced from 0.25 to 0.19 d.b. for avoiding the growth of microorganisms (Rahman, 2007).

Our findings were similar to those found in previous work for tilapia viscera (Camaño Echavarría et al., 2021) and other protein hydrolysates, for instance from okara (Justus et al., 2021), mussel meat (Silva et al., 2012), and chicken meat (Kurozawa et al., 2009). Nevertheless, different results were reported when testing hen egg white powder (Rao & Labuza, 2012), whey powder (Zhou et al., 2014), and rice (Gomes & Kurozawa, 2021) protein hydrolysates. These studies obtained sigmoid-shaped (type II) isotherms, in which  $X_E$  increases with the increase of  $a_W$ , characteristic of starchy food (Carmo & Pena, 2019). The flattening observed when comparing type II with type III isotherm is associated with the number of hydroxyl groups. Whether there are more accessible hydroxyl groups to bind water, the weaker the interactions and the higher the molecular relaxation mechanisms will be (Verruck et al., 2018). The different results may be related to the desorption curves which are influenced by huge features (e.g., composition, structure, and treatments of the material) (Chen et al., 2017).

Concerning Figure 2, it could be observed that, as the temperature was reduced,  $X_E$  of the protein hydrolysate of NT slaughtering by-product increased. It happens, once lower temperatures imply less kinetic energy and, therefore, the molecules bond to the solid with higher strength (Kuenzel & Ranjbar, 2019). In the experiments, there was an increase of 15 °C between each experimental temperature. However, the gap observed between the curve obtained for a lower temperature, 20 °C, and the other curves, 35 °C, and 50 °C was more accentuated. This indicated that, at a lower temperature,  $X_E$  of the protein hydrolysate of NT slaughtering by-product was more influenced by temperature. As the temperature increased, however, its influence was reduced.

Based on our results, we can affirm that the White and Eyring model can be applied as a powerful tool for predicting the stability and moisture behavior during the drying and storage process of NT slaughtering by-product. This knowledge about the suitable sorption isotherm of materials susceptible to deterioration, like NT slaughtering by-product, is crucial for avoiding chemical and biochemical undesirable losses (e.g., color, texture, odor, and taste). For the White and Eyring model, the parameters A and B were adjusted as a logarithm equation and presented a well-defined behavior as a function of temperature. In Figure 3 is showed the relationship of the parameters to the temperature.

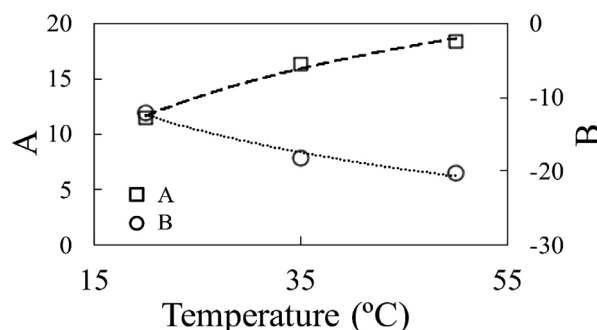


Figure 3. A and B White and Eyring model parameters.

It can be seen from Figure 3 that parameter A was positively influenced by the increase in temperature, in contrast to parameter B, which decreased with the increase in experimental temperature. The adjustments obtained for the parameters of the White and Eyring model as a function of temperature, with  $R^2$  greater than 0.970, are represented by Equations 4 and 5:

$$A = 7.669 \ln(T) - 11.331 \quad (4)$$

$$B = -9,08 \ln(T) + 14.835 \quad (5)$$

Thus, the White and Eyring model with the Equations 4 and 5, can be applied to predict the  $X_E$  of the NT slaughtering by-product protein hydrolysate in the temperature range of 20 °C to 50 °C. This type of approximation is useful when predicting the sample behavior under nontested temperature. For example, in simulation, design, optimization, and control of drying process in which the temperature varies with the time, that are common in the industry. In these applications, the sorption isotherms added with a kinetic mathematical model may represent the best operational conditions based on an objective function.



The total heat of desorption,  $Q_{st}$ , and the net isosteric heat of desorption,  $q_{st}$ , both calculated with Othmer's relation and White and Eyring model, as well as the latent heat of vaporization of pure water,  $\lambda_V$ , are displayed in Figure 4.

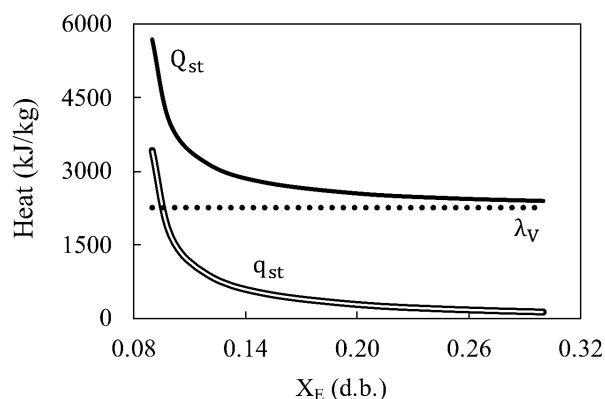


**Figure 4.** Net isosteric heat of desorption,  $q_{st}$  (kJ/kg), total heat of desorption,  $Q_{st}$  (kJ/kg), and latent heat of vaporization of pure water,  $\lambda_V$  (kJ/kg).

Regarding Figure 4, it is observed that with the increase in the  $X_E$  the total heat of desorption,  $Q_{st}$ , approaches the vaporization heat for pure water,  $\lambda_V$ . This behavior is due to the weakening of the bonding energy between the water molecules in the liquid state. When the by-product presented lower  $X_E$ , the interaction energy between the water molecules and the first layer of desorption was bigger than the energy that keeps the molecules together on the successive layers (Wan et al., 2016).

An exponential relation was used to adjust  $Q_{st}$  as a function of  $X_E$ . With an  $R^2$  of 0.994, the equation obtained was represented by Equation 6:

$$Q_{st} = 2454.22 + 3.82\exp(0.605/X_E) \quad (6)$$

The calculated  $Q_{st}$  ranged from 2395 to 5682 kJ/kg, respectively, for  $X_E$  of 0.09 and 0.3 (d.b.). Similar value order of  $Q_{st}$  was achieved in literature, such as for sardine muscles, ~2692 to ~3742 kJ/kg (Djendoubi et al., 2009), frozen raw pork meat, ~2200 to ~3600 kJ/kg (Clemente et al., 2009), fresh beef, ~2200 to ~4700 kJ/kg (Ahmat et al., 2014), and tilapia viscera, 2422 to 3083 kJ/kg (Camaño Echavarría et al., 2021).

The amount of required energy to remove 1 kg of water was inversely proportional to  $X_E$ . At  $X_E < 0.14$  d.b., it could be seen a slight change of  $X_E$  that significantly raised the desorption heat. In this sense, there is significant biochemical stability of the protein hydrolysate under low  $a_w$ . This result is associated with the reduction in the heat of desorption which is synonymous with less biochemical stability of protein hydrolysate, due to the greater  $a_w$ , which implies the activation of enzymes and the development of microorganisms that degrade food (Lavelli et al., 2017).

The lower the  $a_w$  as well as the lower  $X_E$ , as confirmed by the desorption isotherms in Figure 2, the greater will be the energy required to remove the moisture present in the solid matrix. These results are in agreement with the ones verified for protein hydrolysate of anchovy fillet (Moraes & Pinto, 2012). It was observed that small additions on the  $X_E$  entailed great decreases in the desorption heat. This fact can be explained by the existence of a greater quantity of not bonded water when the amounts of water are greater. As the moisture decreases, the amount of free water also decreases, therefore the energy required for evaporation increases. The amount of energy required becomes not only that one required for simple evaporation, but also the one required to break the bonding between water and solid matrix (Bahar et al., 2017).

## 4 Conclusion

In this paper, desorption isotherm and isosteric heat of desorption of NT slaughtering by-product were evaluated. The desorption isotherms were determined by the dynamical model, under temperature conditions of 20 °C, 35 °C,

and 50 °C. Eight models were tested to describe the relationship between the equilibrium moisture content and the water activity. All the desorption isotherm was type III and the empirical model of White and Eyring was the best in predicting the experimental data,  $R^2$  of 0.987. The isosteric heat of desorption, obtained using Othmer's equation, ranged from 2395 to 5682 kJ/kg, for equilibrium moisture content between 0.09 and 0.3 kg/kg. At equilibrium moisture content below 0.14 d.b., slight changes in the moisture implied significant raises in the heat of desorption. An exponential equation was adjusted to relate the isosteric heat of desorption with the equilibrium moisture content. The obtained results can be employed in drying projects, filling the gap in predicting the energy demand and the suitable storage condition of NT slaughtering by-product. Thus, our results represent a useful contribution to realizing the kinetic drying of NT slaughtering by-product as well as the process design.

## References

- Ahmat, T., Bruneau, D., Kuitche, A., & Waste Aregba, A. (2014). Desorption isotherms for fresh beef: An experimental and modeling approach. *Meat Science*, *96*(4), 1417-1424. PMID:24398001. <http://dx.doi.org/10.1016/j.meatsci.2013.12.009>
- Al-Deghayem, W. A., Al-Balawi, H. F., Kandeal, S. A., & Suliman, E. A. M. (2017). Gonadosomatic index and some hematological parameters in African catfish *Clarias gariepinus* (Burchell, 1822) as affected by feed type and temperature level. *Brazilian Archives of Biology and Technology*, *60*, 1-10. <http://dx.doi.org/10.1590/1678-4324-2017160157>
- Association of Official Analytical Chemists – AOAC. (1995). *Official methods of analysis of the Association of Official Analytical Chemists*. Gaithersburg: AOAC.
- Bahar, R., Azzouz, S., Remond, R., Ouertani, S., Elaieb, M. T., & El Cafci, M. A. (2017). Moisture sorption isotherms and thermodynamic properties of Oak wood (*Quercus robur* and *Quercus canariensis*): Optimization of the processing parameters. *Heat and Mass Transfer*, *53*(5), 1541-1552. <http://dx.doi.org/10.1007/s00231-016-1916-0>
- Bastoğlu, A. Z., Koç, M., & Ertekin, F. K. (2017). Moisture sorption isotherm of microencapsulated extra virgin olive oil by spray drying. *Journal of Food Measurement and Characterization*, *11*(3), 1295-1305. <http://dx.doi.org/10.1007/s11694-017-9507-4>
- Blahovec, J., & Yanniotis, S. (2009). Modified classification of sorption isotherms. *Journal of Food Engineering*, *91*(1), 72-77. <http://dx.doi.org/10.1016/j.jfoodeng.2008.08.007>
- Botelho, F. M., Boschiroli Neto, N. J., Botelho, S. C. C., Oliveira, G. H. H., & Hauth, M. R. (2019). Sorption isotherms of Brazil nuts. *Revista Brasileira de Engenharia Agrícola e Ambiental*, *23*(10), 776-781. <http://dx.doi.org/10.1590/1807-1929/agriambi.v23n10p776-781>
- Brooker, D. B., Bakker-Arkema, F. W., & Hall, C. W. (1992). *Drying and storage of grains and oilseeds*. USA: Springer.
- Brunauer, S., Deming, L. S., Deming, W. E., & Teller, E. (1940). On a theory of the van der Waals adsorption of gases. *Journal of the American Chemical Society*, *62*(7), 1723-1732. <http://dx.doi.org/10.1021/ja01864a025>
- Brunauer, S., Emmett, P. H., & Teller, E. (1938). Adsorption of gases in multimolecular layers. *Journal of the American Chemical Society*, *60*(2), 309-319. <http://dx.doi.org/10.1021/ja01269a023>
- Camaño Echavarría, J. A., Rivera Torres, A. M., & Zapata Montoya, J. E. (2021). Sorption isotherms and thermodynamic properties of the dry silage of red tilapia viscera (*Oreochromis* spp.) obtained in a direct solar dryer. *Heliyon*, *7*(4), e06798. PMID:33981880. <http://dx.doi.org/10.1016/j.heliyon.2021.e06798>
- Candido, L. M. B., & Sgarbieri, V. C. (2003). Enzymatic hydrolysis of Nile tilapia (*Oreochromis niloticus*) myofibrillar proteins: Effects on nutritional and hydrophilic properties. *Journal of the Science of Food and Agriculture*, *83*(9), 937-944. <http://dx.doi.org/10.1002/jsfa.1419>
- Carmo, J. R., & Pena, R. da S. (2019). Influence of the temperature and granulometry on the hygroscopic behavior of tapioca flour. *CYTA: Journal of Food*, *17*(1), 900-906. <http://dx.doi.org/10.1080/19476337.2019.1668860>
- Caurie, M. (1970). A new model equation for predicting safe storage moisture levels for optimum stability of dehydrated foods. *International Journal of Food Science & Technology*, *5*(3), 301-307. <http://dx.doi.org/10.1111/j.1365-2621.1970.tb01571.x>
- Chabbouh, M., Sahli, A., & Bellagha, S. (2013). Does the spicing step affect the quality and drying behaviour of traditional kaddid, a tunisian cured meat? *Journal of the Science of Food and Agriculture*, *93*(14), 3634-3641. PMID:23893302. <http://dx.doi.org/10.1002/jsfa.6319>
- Chen, Q., Bi, Y., Bi, J., Zhou, L., Wu, X., & Zhou, M. (2017). Glass Transition and State Diagram for Jujube Powders With and Without Maltodextrin Addition. *Food and Bioprocess Technology*, *10*(9), 1606-1614. <http://dx.doi.org/10.1007/s11947-017-1927-y>
- Chirife, J., & Iglesias, H. A. (1978). Equations for fitting water sorption isotherms of foods. Part 1: A review. *International Journal of Food Science & Technology*, *13*(3), 159-174. <http://dx.doi.org/10.1111/j.1365-2621.1978.tb00792.x>
- Clemente, G., Bon, J., Benedito, J., & Mulet, A. (2009). Desorption isotherms and isosteric heat of desorption of previously frozen raw pork meat. *Meat Science*, *82*(4), 413-418. PMID:20416696. <http://dx.doi.org/10.1016/j.meatsci.2009.02.020>
- Desai, A. S., Brennan, M. A., & Brennan, C. S. (2018). Amino acid and fatty acid profile and digestible indispensable amino acid score of pasta fortified with salmon (*Oncorhynchus tshawytscha*) powder. *European Food Research and Technology*, *244*(10), 1729-1739. <http://dx.doi.org/10.1007/s00217-018-3085-5>
- Dieterich, F., Boscolo, W. R., Bertoldo, M. T. P., Silva, V. S. N., Gonçalves, G. S., & Vidotti, R. M. (2014). Development and characterization of protein hydrolysates originated from animal agro industrial byproducts. *Journal of Dairy, Veterinary & Animal Research*, *1*(2), 56-61. <http://dx.doi.org/10.15406/jdvar.2014.01.00012>
- Djendoubi, N., Boudhrioua, N., Bonazzi, C., & Kechaou, N. (2009). Drying of sardine muscles: Experimental and mathematical investigations. *Food and Bioprocess Technology*, *87*(2), 115-123. <http://dx.doi.org/10.1016/j.fbp.2008.07.003>

- Feltes, M. M. C., Correia, J. F. G., Beirão, L. H., Block, J. M., Ninow, J. L., & Spiller, V. R. (2010). Alternativas para a agregação de valor aos resíduos da industrialização de peixe. *Revista Brasileira de Engenharia Agrícola e Ambiental*, 14(6), 669-677. <http://dx.doi.org/10.1590/S1415-43662010000600014>
- Food and Agriculture Organization of the United Nations – FAO. (2020). *The State of World Fisheries and Aquaculture 2020. Sustainability in action*. Rome: FAO. <https://doi.org/10.4060/ca9229en>
- Galdeano, M. C., Tonon, R. V., Carvalho, C. W. P., Menezes, N. S., Nogueira, R. I., Leal-Junior, W. F., & Minguita, A. P. S. (2018). Moisture sorption isotherms of raw and extruded wholemeal sorghum flours studied by the dynamic and salt slurry methods. *Brazilian Journal of Food Technology*, 21(0), <http://dx.doi.org/10.1590/1981-6723.20717>
- Gomes, M. H. G., & Kurozawa, L. E. (2021). Influence of rice protein hydrolysate on lipid oxidation stability and physico-chemical properties of linseed oil microparticles obtained through spray-drying. *LWT - Food Science and Technology*, 139, 110510. <https://doi.org/10.1016/j.lwt.2020.110510>
- Ibarz, A., & Barbosa-Canovas, G. V. (2014). *Introduction to food process engineering*. London: Taylor & Francis Group.
- Jian, F., & Jayas, D. S. (2021). *Grains: Engineering fundamentals of drying and storage*. Boca Raton: CRC Press. <http://dx.doi.org/10.1201/9781003186199>
- Justus, A., Ida, E. I., & Kurozawa, L. E. (2021). Microencapsulation of okara protein hydrolysate by spray drying: Physicochemical and nutritive properties, sorption isotherm, and glass transition temperature. *Drying Technology*, 1, 1-12. <http://dx.doi.org/10.1080/07373937.2021.1920031>
- Khan, A. A., Hossain, A., Hara, K., Osatomi, K., Ishihara, T., & Nozaki, Y. (2003). Effect of enzymatic fish protein hydrolysate from fish scrap on the state of water and denaturation of lizard fish (*Saurida wanieso*) myofibrils during dehydration. *Food Science and Technology Research*, 9(3), 257-263. <http://dx.doi.org/10.3136/fstr.9.257>
- Kobayashi, Y., & Park, J. W. (2018). Optimal blending of differently refined fish proteins based on their functional properties. *Journal of Food Processing and Preservation*, 42(1), 1-9. <http://dx.doi.org/10.1111/jfpp.13346>
- Kuenzel, C., & Ranjbar, N. (2019). Dissolution mechanism of fly ash to quantify the reactive aluminosilicates in geopolymerisation. *Resources, Conservation and Recycling*, 150, 1-10. <http://dx.doi.org/10.1016/j.resconrec.2019.104421>
- Kurozawa, L. E., Park, K. J., & Hubinger, M. D. (2009). Effect of maltodextrin and gum arabic on water sorption and glass transition temperature of spray dried chicken meat hydrolysate protein. *Journal of Food Engineering*, 91(2), 287-296. <http://dx.doi.org/10.1016/j.jfoodeng.2008.09.006>
- Langmuir, I. (1916). The constitution and fundamental properties of solids and liquids. *Journal of the American Chemical Society*, 38(11), 2221-2295. <http://dx.doi.org/10.1021/ja02268a002>
- Lavelli, V., Sri Harsha, P. S. C., Laureati, M., & Pagliarini, E. (2017). Degradation kinetics of encapsulated grape skin phenolics and micronized grape skins in various water activity environments and criteria to develop wide-ranging and tailor-made food applications. *Innovative Food Science & Emerging Technologies*, 39, 156-164. <http://dx.doi.org/10.1016/j.ifset.2016.12.006>
- Leuk, P., Schneeberger, M., Hirn, U., & Bauer, W. (2016). Heat of sorption: A comparison between isotherm models and calorimeter measurements of wood pulp. *Drying Technology*, 34(5), 563-573. <http://dx.doi.org/10.1080/07373937.2015.1062391>
- Marques, B. C., Rayo-Mendez, L. M., & Tadini, C. C. (2022). Applying the concept of state diagram on the stability analysis of an NSP-rich ingredient extracted from overripe bananas (*Musa cavendishii* var. Nanicaõ). *Food Chemistry*, 367, 130639. <https://doi.org/10.1016/j.foodchem.2021.130639>
- Miranda, J. C., Mazzoni, R., Eduardo, C., & Silva, A. (2010). Occurrence of Nile Tilapia *Oreochromis niloticus* Linnaeus, 1758 at microbasin of Mato Grosso River, Saquarema, Rio de Janeiro. *SaBios-Revista de Saúde e Biologia*, 5(2), 47-50.
- Moraes, K., & Pinto, L. A. A. (2012). Desorption isotherms and thermodynamics properties of anchovy in natura and enzymatic modified paste. *Journal of Food Engineering*, 110(4), 507-513. <http://dx.doi.org/10.1016/j.jfoodeng.2012.01.012>
- Moreira, R., Chenlo, F., Vázquez, M. J., & Cameán, P. (2005). Sorption isotherms of turnip top leaves and stems in the temperature range from 298 to 328 K. *Journal of Food Engineering*, 71(2), 193-199. <http://dx.doi.org/10.1016/j.jfoodeng.2004.10.033>
- Oliveira, D. E. C., Resende, O., Costa, L. M., Silva, G. P., & Sales, J. de F. (2017). Hygroscopicity of 'sucupira-branca' (*Pterodon emarginatus* vogel) fruits. *Revista Brasileira de Engenharia Agrícola e Ambiental*, 21(4), 285-289. <http://dx.doi.org/10.1590/1807-1929/agriambi.v21n4p285-289>
- Othmer, D. F., & Brown, G. G. (1940). Correlating vapor pressure and latent heat data. *Industrial & Engineering Chemistry*, 32(6), 841-856. <https://doi.org/10.1021/ie50366a022>
- Oswin, C. R. (1946). The kinetics of package life. III. The isotherm. *Journal of the Society of Chemical Industry*, 65(12), 419-421. <http://dx.doi.org/10.1002/jctb.5000651216>
- Rahman, M. S. (2007). *Handbook of food preservation* (2nd ed.). Boca Raton: CRC Press. <http://dx.doi.org/10.1201/9781420017373>
- Rao, Q., & Labuza, T. P. (2012). Effect of moisture content on selected physicochemical properties of two commercial hen egg white powders. *Food Chemistry*, 132(1), 373-384. PMID:26434304. <http://dx.doi.org/10.1016/j.foodchem.2011.10.107>
- Schössler, K., Jäger, H., & Knorr, D. (2012). Effect of continuous and intermittent ultrasound on drying time and effective diffusivity during convective drying of apple and red bell pepper. *Journal of Food Engineering*, 108(1), 103-110. <http://dx.doi.org/10.1016/j.jfoodeng.2011.07.018>
- Shu, C. H., & Tsai, C. C. (2016). Enhancing oil accumulation of a mixed culture of *Chlorella* sp. and *Saccharomyces cerevisiae* using fish waste hydrolysate. *Journal of the Taiwan Institute of Chemical Engineers*, 67, 377-384. <http://dx.doi.org/10.1016/j.jtice.2016.08.022>
- Silva, V. M., Kurozawa, L. E., Park, K. J., & Hubinger, M. D. (2012). Water sorption and glass transition temperature of spray-dried mussel meat protein hydrolysate. *Drying Technology*, 30(2), 175-184. <http://dx.doi.org/10.1080/07373937.2011.628766>
- Smith, S. E. (1947). The sorption of water vapor by high polymers. *Journal of the American Chemical Society*, 69(3), 646-651. <https://doi.org/10.1021/ja01195a053>

- Toujani, M., Hassini, L., Azzouz, S., & Belghith, A. (2011). Drying characteristics and sorption isotherms of silverside fish (*Atherina*). *International Journal of Food Science & Technology*, 46(3), 594-600. <http://dx.doi.org/10.1111/j.1365-2621.2010.02524.x>
- Van der Berg, C., & Bruin, S. (1981). *Water activity: Influence on food quality*. New York: Academic Press.
- Verruck, S., Santana, F., de Olivera Müller, C., & Prudencio, E. S. (2018). Thermal and water sorption properties of Bifidobacterium BB-12 microcapsules obtained from goat's milk and prebiotics. *Lebensmittel-Wissenschaft + Technologie*, 98, 314-321. <http://dx.doi.org/10.1016/j.lwt.2018.08.060>
- Wan, K., He, Q., Miao, Z., Liu, X., & Huang, S. (2016). Water desorption isotherms and net isosteric heat of desorption on lignite. *Fuel*, 171, 101-107. <http://dx.doi.org/10.1016/j.fuel.2015.12.054>
- Wani, S. A., & Kumar, P. (2016). Moisture sorption isotherms and evaluation of quality changes in extruded snacks during storage. *Lebensmittel-Wissenschaft + Technologie*, 74, 448-455. <http://dx.doi.org/10.1016/j.lwt.2016.08.005>
- White, H. J. J., & Eyring, H. (1947). The adsorption of water by swelling high polymeric materials. *Textile Research Journal*, 17, 523-553. <http://dx.doi.org/10.1177/004051754701701001>
- Zapata, J. I. H., & De La Pava, G. C. R. (2018). Physicochemical analysis of frankfurter type sausages made with red tilapia fillet waste (*Oreochromis* sp) and quinoa flour (*Chenopodium quinoa* W.). *Brazilian Journal of Food Technology*, 21, e2016103. <http://dx.doi.org/10.1590/1981-6723.10316>
- Zhang, N., Yamashita, Y., & Nozaki, Y. (2002). Effect of protein hydrolysate from Antarctic krill meat on the state of water and denaturation by dehydration of lizard fish myofibrils. *Fisheries Science*, 68(3), 672-679. <http://dx.doi.org/10.1046/j.1444-2906.2002.00476.x>
- Zhou, P., Liu, D., Chen, X., Chen, Y., & Labuza, T. P. (2014). Stability of whey protein hydrolysate powders: Effects of relative humidity and temperature. *Food Chemistry*, 150, 457-462. PMID:24360475. <http://dx.doi.org/10.1016/j.foodchem.2013.11.027>

---

**Funding:** Coordenação de Aperfeiçoamento de Pessoal de Nível Superior - Brasil (CAPES) - (proj. 001).

---

Received: Nov. 27, 2021; Accepted: June 12, 2022

Associate Editor: Rosinelson da Silva Pena.